Fast scanning peripheral wave-front sensor for the human eye

Bart Jaeken,[1,*] Linda Lundström,[2] and Pablo Artal[1]

[1]*Laboratorio de Óptica, Universidad de Murcia, Campus Espinardo (Ed. CiOyN), Murcia, Spain*
[2]*Biomedical and X-Ray Physics, Royal Institute of Technology, Stockholm, Sweden*
**bart.jaeken@um.es*

Abstract: We designed and built a fast scanning peripheral Hartmann-Shack (HS) wave-front sensor to measure the off-axis wave-front aberrations in the human eye. The new instrument is capable of measuring the optical quality over the central 80° horizontal visual field in 1.8 seconds with an angular resolution of 1°. The subject has an open field of view without any moving elements in the line-of-sight and the head is kept in place by a head-chin rest. The same efficiency, reliability and measurement quality as the current static HS sensor were found but with much higher acquisition speed and comfort for the patients. This instrument has the potential to facilitate and improve future research on the peripheral optical quality of the eye in large groups of subjects.

OCIS codes: (120.5800) Scanners; (330.7325) Visual optics, metrology; (330.7310) Vision.

References and links

1. F. Rempt, J. Hoogerheide, and W. P. H. Hoogenboom, "Peripheral retinoscopy and the skiagram," Ophthalmologica **162**(1), 1–10 (1971).
2. R. Navarro, P. Artal, and D. R. Williams, "Modulation transfer of the human eye as a function of retinal eccentricity," J. Opt. Soc. Am. A **10**(2), 201–212 (1993).
3. A. Guirao and P. Artal, "Off-axis monochromatic aberrations estimated from double pass measurements in the human eye," Vision Res. **39**(2), 207–217 (1999).
4. D. R. Williams, P. Artal, R. Navarro, M. J. McMahon, and D. H. Brainard, "Off-axis optical quality and retinal sampling in the human eye," Vision Res. **36**(8), 1103–1114 (1996).
5. L. Lundström, A. Mira-Agudelo, and P. Artal, "Peripheral optical errors and their change with accommodation differ between emmetropic and myopic eyes," J. Vis. **9**(6), 17, 1–11 (2009).
6. J. Hoogerheide, F. Rempt, and W. P. H. Hoogenboom, "Acquired myopia in young pilots," Ophthalmologica **163**(4), 209–215 (1971).
7. W. N. Charman and H. Radhakrishnan, "Peripheral refraction and the development of refractive error: a review," Ophthalmic Physiol. Opt. **30**(4), 321–338 (2010).
8. L. Lundström, J. Gustafsson, and P. Unsbo, "Vision evaluation of eccentric refractive correction," Optom. Vis. Sci. **84**(11), 1046–1052 (2007).
9. J. Gustafsson and P. Unsbo, "Eccentric correction for off-axis vision in central visual field loss," Optom. Vis. Sci. **80**(7), 535–541 (2003).
10. A. V. Goncharov, M. Nowakowski, M. T. Sheehan, and C. Dainty, "Reconstruction of the optical system of the human eye with reverse ray-tracing," Opt. Express **16**(3), 1692–1703 (2008).
11. X. Wei and L. Thibos, "Modeling the eye's optical system by ocular wavefront tomography," Opt. Express **16**(25), 20490–20502 (2008).
12. P. Artal, A. M. Derrington, and E. Colombo, "Refraction, aliasing, and the absence of motion reversals in peripheral vision," Vision Res. **35**(7), 939–947 (1995).
13. Y. Z. Wang, L. N. Thibos, and A. Bradley, "Effects of refractive error on detection acuity and resolution acuity in peripheral vision," Invest. Ophthalmol. Vis. Sci. **38**(10), 2134–2143 (1997).
14. L. Lundström, S. Manzanera, P. M. Prieto, D. B. Ayala, N. Gorceix, J. Gustafsson, P. Unsbo, and P. Artal, "Effect of optical correction and remaining aberrations on peripheral resolution acuity in the human eye," Opt. Express **15**(20), 12654–12661 (2007).
15. H. Hofer, P. Artal, B. Singer, J. L. Aragon, and D. R. Williams, "Dynamics of the eye wave aberrations," J. Opt. Soc. Am. A **18**(3), 497–506 (2001).
16. H. Radhakrishnan and W. N. Charman, "Peripheral refraction measurement: does it matter if one turns the eye or the head?" Ophthalmic Physiol. Opt. **28**(1), 73–82 (2008).
17. P. Prado, J. Arines, S. Bará, S. Manzanera, A. Mira-Agudelo, and P. Artal, "Changes of ocular aberrations with gaze," Ophthalmic Physiol. Opt. **29**(3), 264–271 (2009).

#140615 - $15.00 USD Received 5 Jan 2011; revised 23 Mar 2011; accepted 25 Mar 2011; published 8 Apr 2011

18. J. Tabernero and F. Schaeffel, "Fast scanning photoretinoscope for measuring peripheral refraction as a function of accommodation," J. Opt. Soc. Am. A **26**(10), 2206–2210 (2009).
19. X. Wei and L. Thibos, "Design and validation of a scanning Shack Hartmann aberrometer for measurements of the eye over a wide field of view," Opt. Express **18**(2), 1134–1143 (2010).
20. R. D. Ferguson, Z. Zhong, D. X. Hammer, M. Mujat, A. H. Patel, C. Deng, W. Zou, and S. A. Burns, "Adaptive optics scanning laser ophthalmoscope with integrated wide-field retinal imaging and tracking," J. Opt. Soc. Am. A **27**(11), A265–A277 (2010).
21. D. A. Atchison, N. Pritchard, and K. L. Schmid, "Peripheral refraction along the horizontal and vertical visual fields in myopia," Vision Res. **46**(8-9), 1450–1458 (2006).
22. P. M. Prieto, F. Vargas-Martín, S. Goelz, and P. Artal, "Analysis of the performance of the Hartmann-Shack sensor in the human eye," J. Opt. Soc. Am. A **17**(8), 1388–1398 (2000).
23. L. Lundström and P. Unsbo, "Unwrapping Hartmann-Shack images from highly aberrated eyes using an iterative B-spline based extrapolation method," Optom. Vis. Sci. **81**(5), 383–388 (2004).
24. L. Lundström, J. Gustafsson, and P. Unsbo, "Population distribution of wavefront aberrations in the peripheral human eye," J. Opt. Soc. Am. A **26**(10), 2192–2198 (2009).
25. L. Lundström and P. Unsbo, "Transformation of Zernike coefficients: scaled, translated, and rotated wavefronts with circular and elliptical pupils," J. Opt. Soc. Am. A **24**(3), 569–577 (2007).
26. J. Santamaría, P. Artal, and J. Bescós, "Determination of the point-spread function of human eyes using a hybrid optical-digital method," J. Opt. Soc. Am. A **4**(6), 1109–1114 (1987).
27. C. Fedtke, F. Manns, and A. Ho, "The entrance pupil of the human eye: a three-dimensional model as a function of viewing angle," Opt. Express **18**(21), 22364–22376 (2010).

1. Introduction

The interest in measuring the peripheral optical quality of the eye [1–5] has increased ever since the suggestion that a relative peripheral hyperopia may be a cue to develop myopia [6,7]. But beyond myopia research, other areas also require information on the off-axis optical quality. For example the investigation of central vision field loss [8,9], eye modelling with individual data retrieved from ocular wavefront tomography [10,11], and the effect of optical errors on peripheral vision [12–14].

Because the eye is an optical system that is subject to dynamic variation [15], fast measurements are always better. But the availability of instruments measuring the peripheral optical quality in a fast and reliable manner is limited. Commercially available auto-refractors with an open field of view were used by modifying the fixation target and thus having the subject to turn the eye in different angles. Although the effect of turning the eye has been considered to be negligible [16,17], data acquisition time remains a limiting factor and can have a negative influence when comparing data from different angles, especially when measuring eyes that are not under cycloplegia. To reduce the acquisition time and to improve the comfort of the subject, a scanning instrument is necessary, where the instrument is moving relative to the subject, as opposed to a static instrument, where the subject has to turn the eye during the series of measurements.

To our knowledge only two scanning instruments for measuring off-axis refraction exist today [18,19]. The scanning photo-retinoscope [18] measures the refractive power of the eye over the horizontal meridian with high speed, scanning range, and angular resolution. The scanning Hartmann-Shack (HS) wavefront sensor [19] measures the wavefront aberrations of the eye at 37 points over the central 30° visual field. It may be also possible to use wide angle scanning laser ophthalmoscopes equipped with adaptive optics to infer peripheral aberrations [20].

In this article, we describe a new design of a peripheral wavefront scanner which combines the high speed, resolution, and range of the photo-retinoscope instrument with the ability to measure the whole wavefront and precision of HS wavefront sensor. A rotational movement forms the base of the scanner ensuring equal distances between the eye and the sensor at all times. The characteristics (open field of view for the subject, simplicity of handling and high speed acquisition) of our custom-built fast scanning HS offer a reliable use in a clinic and in large population studies. The following sections describe in detail the instrument and its validation by comparing it to a static HS system [5] for 9 subjects measured over 80° of the horizontal visual field.

#140615 - $15.00 USD Received 5 Jan 2011; revised 23 Mar 2011; accepted 25 Mar 2011; published 8 Apr 2011

2. Methods

2.1 Instrument design specifications

The specifications of the instrument in speed, scanning range, and resolution were optimized to investigate peripheral optics easily in large groups of subjects. Current studies on peripheral image quality [21] have demonstrated that the horizontal meridian presents the most variation of the relative peripheral refractive error. Therefore, when studying myopia development, this meridian is often chosen [6]. The larger the measuring range over the horizontal visual field, the better. However, when using a HS wavefront sensor the spot pattern starts to degrade rapidly for angles larger than 35°- 40° off-axis due to the large eye's peripheral aberrations. In addition, the pupil appears elliptically shaped when measured off-axis and becomes very narrow. Both factors affect the accuracy of the aberration reconstruction. With static instruments the number of angles is often restricted to minimize the acquisition time. A scanning module gives the possibility to sample at a much higher resolution. Depending on the scope of the study, the angular resolution can easily be changed. The comfort of the subject also has its impact on the quality of the measurements; therefore it was an important design factor.

The instrument was designed to minimize the acquisition time (order of seconds instead of minutes with other approaches), to avoid moving elements in the line-of-sight of the subject, and to use a head-chin rest instead of a bite bar to fixate the eye. It measures the eye's optical quality over the central 80° with an angular resolution of 1 measurement per degree.

2.2 Hardware and settings

Figure 1 shows a schematic view of the instrument and Fig. 2 shows the layout of the instrument. The distance between the pupil plane (*PP*) of the eye and the sensor is critical and should remain equal at all angles (i.e. *PP* is at one focal length distance of lens 2 (*L2*)). This is insured by a rotational movement with the centre of rotation placed in the pupil plane (*PP*). An L-shaped arm contains both the illumination and the measuring optics (*L1*, *L2*, *L3*, *F*, *D*, *BS*, *M1*, *M2*, *ML*, and *C*) and is fixed on the rotation stage. Stationary mirrors (*LM*, 200 x 35 mm, and *HM*) were incorporated in the design to avoid moving elements in the line-of-sight of the subject. A hot mirror (*HM*) allows an open field of view that is reserved for placing a single fixation target.

#140615 - $15.00 USD Received 5 Jan 2011; revised 23 Mar 2011; accepted 25 Mar 2011; published 8 Apr 2011

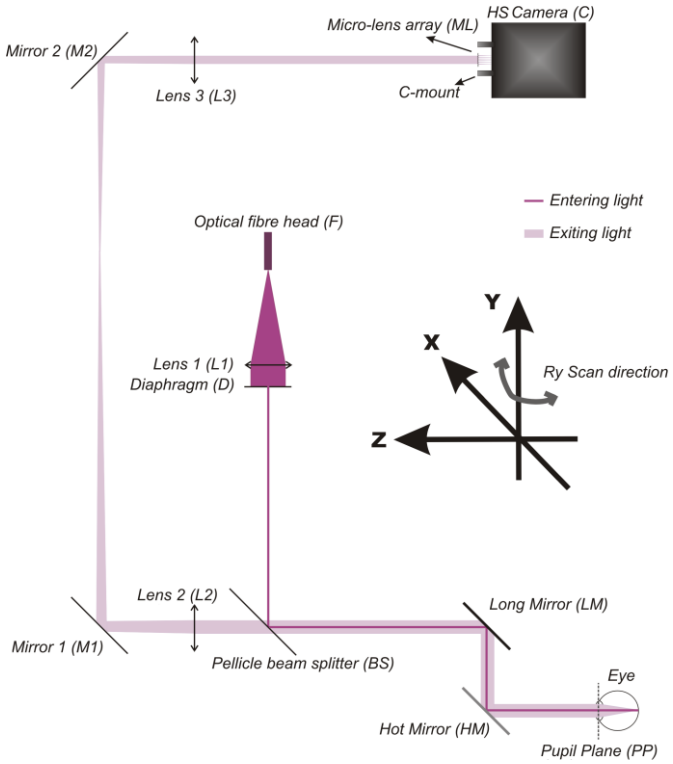

Fig. 1. Schematic side view of the optical design of the HS wavefront sensor scanner.

A DC-Servo motor stage M-061.PD, with a maximum speed of 90°/s, driven by the C-863 Mercury DC-Servo motor controller (Physic Instrumente (PI), Karlsruhe, Germany) provide the rotational movement. The light source is a 780-nm diode laser (model S1FC780, Thorlabs, Newton, USA) and is coupled into the system with an optical fibre (*F*). A diaphragm (*D*) permits to change the diameter of the beam. As in a standard HS sensor for the eye [22], although sequentially, the light reflected on the retina reaches the microlenses array (*ML*) (hexagonal array, 200 µm pitch, and 7 mm focal length) and the camera through one telescope system (*L2-L3*). Fast acquisition is reached with the Genie HM1024 GigE vision compliant CMOS camera (Dalsa, Waterloo, Canada). This camera has a 1024 x 768 pixel array, 8 bit depth and can acquire up to 117 frames per second. Since the motor operates with an USB-cable and the camera uses the Ethernet port of the computer, a standard computer workstation is used. A mechanic frame specially designed to allocate all the necessary components of the instrument is mounted on an ophthalmic XYZ bench with a head-chin rest. This bench makes it possible for the operator to move the whole system to the correct position for measuring (either the left or the right eye) while the subject is in the head-chin rest (see Fig. 2).

#140615 - $15.00 USD Received 5 Jan 2011; revised 23 Mar 2011; accepted 25 Mar 2011; published 8 Apr 2011

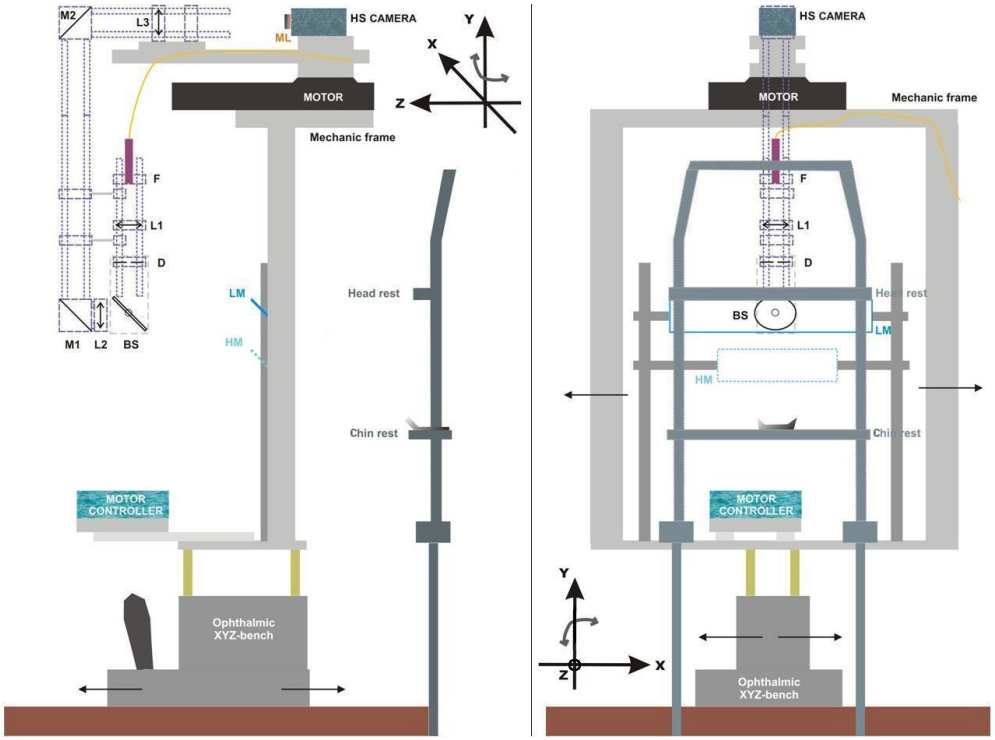

Fig. 2. Schematic side (left) and front (right) view of the HS-scanner showing the layout of the instrument. The arrows show the direction of possible movement of the ophthalmic bench.

The alignment of the subject follows a fixed protocol. For this, two cameras are used. The first rough XYZ-alignment is done with an auxiliary camera (USB-webcam) located on the mechanical frame viewing the face of the subject. Once the light beam enters the eye, fine-tuning is done using the HS-camera. The correct XYZ-position is reached when the HS-image falls on the centre of the CCD of the HS-camera for the checked angles 0° and ± 40°. To avoid the corneal reflex from disturbing the image, the beam has to enter the eye slightly below the corneal apex.

2.3 Software and settings

The data acquisition and user interface are implemented with labVIEW (National Instruments, Austin, USA). The movement of the motor and the data acquisition of the HS-camera are synchronised without stopping the system. The disadvantage of this method is that a measurement is not taken at one specific point; it is the integration of the optical quality over a small area. To ensure that the measurements are separated at least by the same angle as the angle of integration, the integration angle has to be smaller than 0.5°. Some clear advantages of measuring continuously are that the acquisition can be done much faster and that vibrations due to fast stopping and accelerating the system are avoided. Since the exposure time of the camera is short, coherent speckles in the HS image can be a risk, but because of the integration over time and angle, speckle noise was reduced in the HS spot patterns.

The standard capabilities of the instrument are as follows. It scans over an angle of 90°, although to prevent noise due to acceleration and stopping effects of the measuring arm, acquisition is only done over the central 80°. The intensity of the illumination light in the pupil plane is 10 μW/cm^2, a few orders of magnitude below the safety limit standards for this wavelength. The beam entering the eye has a diameter of approximately 1.5 mm. The acquisition time for one frame is 9 ms. The scanning speed is 50°/s and the data acquisition is at 50 Hz. One frame is the integration over 0.45° of visual angle leaving 0.55° of visual angle

#140615 - $15.00 USD Received 5 Jan 2011; revised 23 Mar 2011; accepted 25 Mar 2011; published 8 Apr 2011

between consecutive measurements. Because the change of aberrations in the human eye over one degree of visual angle are small, we assume not to loose resolution that could be of importance. The accuracy of the synchronization between the movement and the data acquisition is better than 1°. Generally four consecutive scans are taken for one eye, resulting in 4 times 81 images (324 HS-images) acquired in 4 times 1.8 seconds (7.2 seconds). Figure 3 is a video of the operation of the instrument in real time.

Data elaboration is automated using MATLAB (MathWorks, Natick, USA). It consists of several steps: spot detection, unwrapping with an iterative b-spline method [23], pupil fitting, Zernike fitting [24], and mathematical rescaling [25]. Images that fail during the firsts steps are immediately discarded. Zernike coefficients are fitted over a circle encircling all measured HS-spots before they are rescaled mathematically to a pupil size smaller than the minor axis of an ellipse fitted around the measured HS-spots. Finally, the four sets of Zernike coefficients in each eccentricity are averaged and the refraction is calculated from the second order terms.

The noise of the system and the variation of the instrumental aberrations with angle were investigated by placing the centre of a manual rotation stage, on which a collimated laser beam was mounted, in *PP*. The intensity of the laser was chosen to illuminate the pixels of the HS-camera in the same range as when measuring in a normal eye. Because of the low resolution of the manual rotation stage the whole angular range (80°) was sampled in steps of 2°. The aberrations of the target angle were the average aberrations measured at 11 equally spaced positions 0.5° around that angle. The entire angular range was scanned five times. The noise of a clinical measurement was checked by comparing the results of the 4 consecutive scans of 10 naïve subject measured under natural condition.

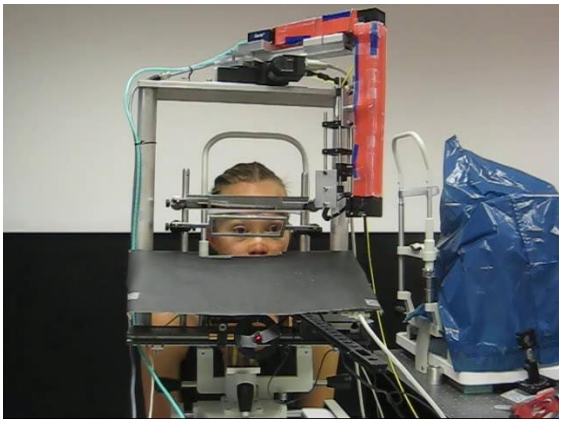

Fig. 3. Shows an example of the operation of the instrument in real time. The video is 1.42 MB, QuickTime mov-format (size 640 x 480) (Media 1).

3. Results

3.1 Calibration of the system

The calibration process consisted of two parts; the determination of the exact magnification of the whole system and the distance between the micro-lens array and the camera (~effective focal length of *ML*), and the creation of the angular reference file.

The determination of the exact magnification and focal length was only done at 0°. A mechanical eye model consisting of a 25.4 mm lens with a rotating diffusing element in the focal plane of the lens and a 6 mm aperture was placed in the pupil plane (*PP*). Trial lenses ranging between ± 6D were placed as close as possible to the principle plane of the model eye. The measured HS-images were elaborated calculating the mean spherical equivalent (*M*) using different values of focal length and magnification to find the best fit with the power of the trial lenses (see Fig. 4). The observed asymmetry is mainly caused by the small variation

#140615 - $15.00 USD Received 5 Jan 2011; revised 23 Mar 2011; accepted 25 Mar 2011; published 8 Apr 2011

in spherical aberration between the different trial lenses. Nevertheless only the range between ± 4 D was used in the optimization process.

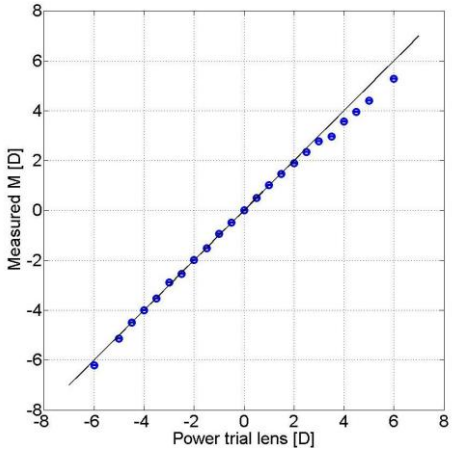

Fig. 4. Calibration of the system using trial lenses. The power of the trial lens is plotted on the X-axis and the measured defocus on the Y-axis. This calibration is only done at 0°.

During unwrapping, the measured HS-image is compared with a reference measurement, which includes the aberrations of the instrument. In a non-scanning system the light always passes through the same part of the optics of the instrument so only one reference image is necessary. Since we want to avoid moving elements in the line-of-sight of the subject, the light is reflected on different parts of the two fixed mirrors (*HM* and *LM*) during the scanning process. The reflection at different locations of the mirrors and the stress on the optical components due to their fixation make the instrumental aberrations vary with eccentricity. This variation with angle is very constant and can therefore be compensated with an angular reference file. Figure 5 shows the angular instrumental error for defocus, astigmatism.

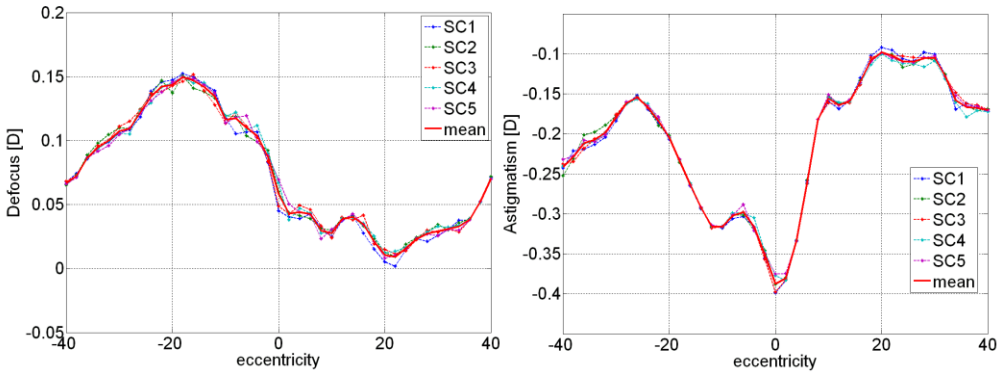

Fig. 5. Instrument aberrations as a function of eccentricity: defocus and astigmatism in diopters. The results of five entire scans are plotted along with the mean of those scans. To compensate this variation, an angular reference file containing the instrumental aberrations is used when elaborating measured data.

The repeatability of the sensor for this perfect situation was high. The average standard deviation for all measured angles is very small: 0.003 D for defocus, 0.004 D for astigmatism and 0.001 µm for higher order RMS for 8 mm pupil. The average standard deviation of the four consecutive scans for all measured angles (except for the area of the optical nerve between 10° and 18°) was calculated for 10 naïve subjects with varying refractive errors (–0.97 ± 1.07 D) to quantify the repeatability of the instrument in a clinical situation: 0.094 D

#140615 - $15.00 USD Received 5 Jan 2011; revised 23 Mar 2011; accepted 25 Mar 2011; published 8 Apr 2011

for defocus, 0.124 D for astigmatism and 0.023 µm for higher order RMS for a 4 mm pupil. The largest noise factor is the degradation of the HS-image due to the large increase of aberrations especially off-axis. In less than 5% of the measured aberrations (2-4th order) of the 10 subjects, the scans were found significant different ($p<0.05$) using a one way ANOVA test.

3.2 Validation of instrument

The validation of the new HS-scanner is done by comparing the measurements with a static HS sensor (described in [5]) for measuring peripheral aberrations in every 10° of visual angle between ± 40°. The right eye of 9 subjects (foveal spherical refractive error of −2.5 ± 2.7 D) was measured. One of the subjects was highly myopic and fell outside the measurable range of the instruments (± 5 D) and was therefore measured with his spectacles. Another subject was on the limit and was measured both with and without correction. The fixation of both systems was a point source placed 2-m away from the subject created by a red laser pointer. For the scanning system the pointer was fixed to the mechanical frame so that the fixation target stayed in the correct position also when moving the frame during alignment of the subject. The instruments were located in different rooms, but in the same building of the laboratory. For most subjects all measurements were taken within a couple of hours to minimize the possible diurnal fluctuations of the eye's optics. All measurements were done under natural conditions without pupil dilation. Informed consent was obtained from all participants prior to the measurements and the study protocol for the use of the instruments and the experiment was in accordance with the guidelines of the Declaration of Helsinki. The results for the mean spherical equivalent (*M*) calculated from the 2nd order Zernike coefficients and the higher order RMS were compared for a pupil size of 4 mm.

Comparison of the measurements taken with the static and the scanning instrument are shown in Fig. 6 for 3 subjects. Figure 7 shows the strong correlation between the results of the mean defocus measured with both instruments, for all subjects (slope = 1.007, R = 0.978 and p = 0.442). The exact angles of the static data set were used in the comparison.

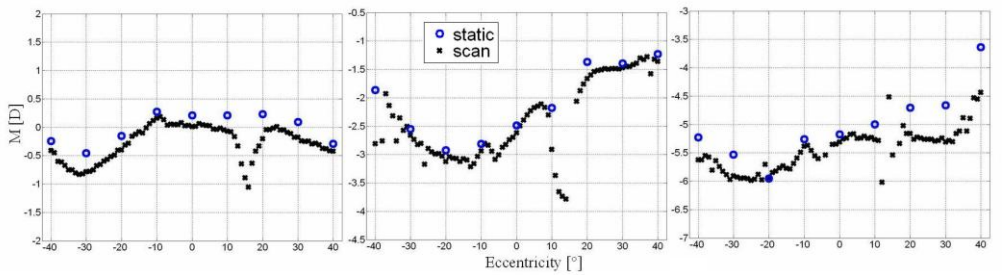

Fig. 6. Comparison of mean spherical equivalent (*M*) between the static system (blue circles) and scanning system (black crosses) for 3 subjects with different refraction. The X-axis contains the eccentricity [°] and the Y-axis *M* [D]. The scale of the Y-axis is for all equal but slightly moved.

#140615 - $15.00 USD Received 5 Jan 2011; revised 23 Mar 2011; accepted 25 Mar 2011; published 8 Apr 2011

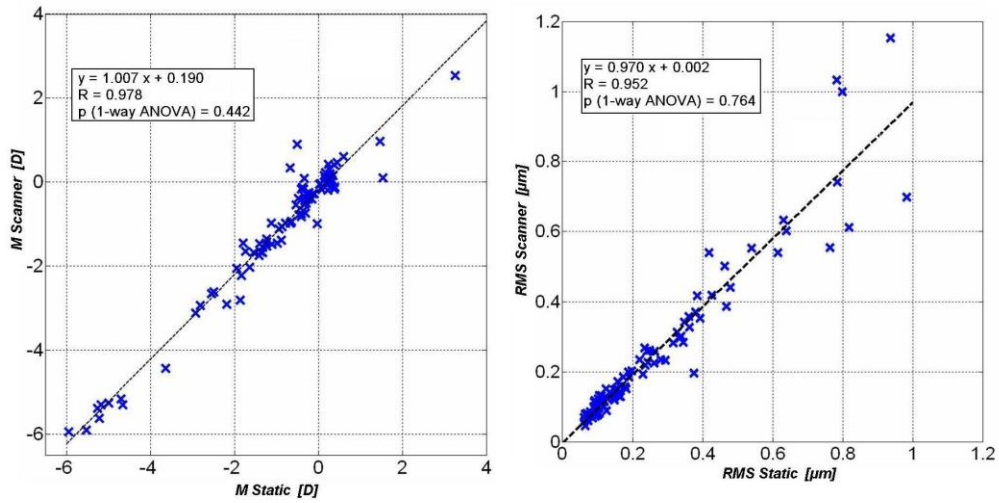

Fig. 7. On the left the correlation plot for all measurements is given with the measured mean sphere (M) of the static system versus that of the scanning system. The right figure shows the correlation plot for all the measured higher order RMS (3rd-4th order, 4 mm pupil) of the static system versus that of the scanning system.

We also found a very good correspondence for the higher order aberrations measured with the static and the scanning instrument. Comparing the results of the higher order RMS (3rd-4th order, 4 mm pupil) measured with both instruments again a strong correlation was found (slope = 0.970, R = 0.952, p = 0.764). The results are shown in Figs. 7 and 8.

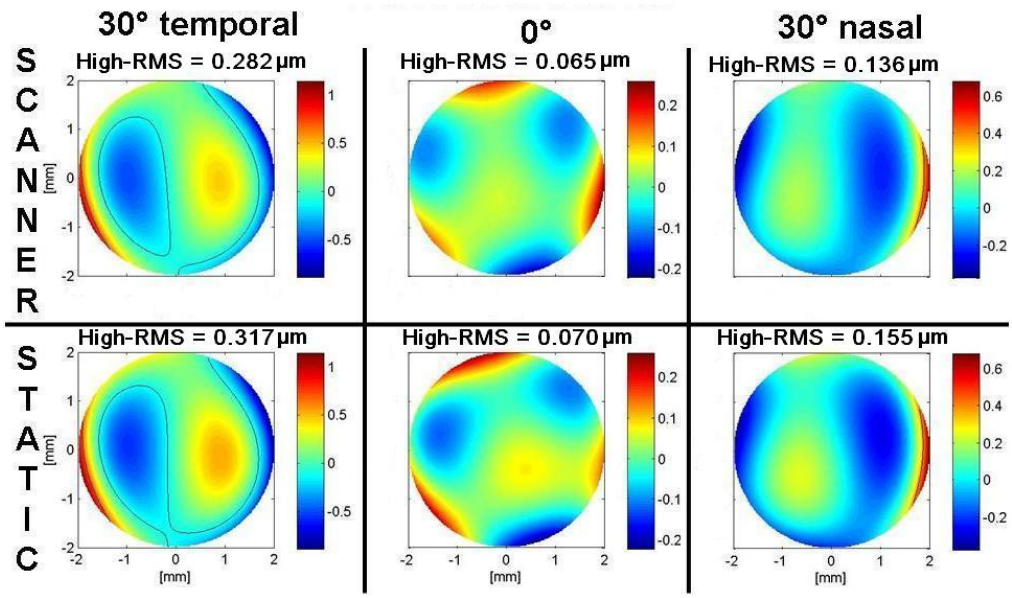

Fig. 8. The wavefront plot of the higher order RMS values measured at three different eccentricities is shown. The values are in µm and are calculated for a 4 mm pupil. Each set of wavefront maps for one eccentricity have the same scale and colour normalization.

The correlation analyses of the aberrations measured with the scanning system and with the static system showed high comparison. Using a one-way ANOVA test the results measured with both instruments were not significant different.

#140615 - $15.00 USD Received 5 Jan 2011; revised 23 Mar 2011; accepted 25 Mar 2011; published 8 Apr 2011

4. Discussion

We designed and built a fast scanning HS wavefront sensor for the periphery. The device scans 80° of the horizontal visual field, acquiring sample data at every degree. Scanning one full meridian takes less than two seconds and even four consecutive measurements are faster than the average break-up time of the tear film. The high measuring speed is reached by the use of a rotational scanning movement, which guarantees a fixed distance between the instrument and the subject's eye. The scanning platform is here used together with a HS-sensor but could also be used in combination with other instruments that measure different ocular characteristics (e.g. a double-pass system [26]).

The comfort of the subject had high priority when designing the instrument. Not only the speed of acquisition and the nearly invisible (780 nm) measuring light are comfortable, but also the use of a head-chin rest and the open field of view, without moving elements in the line-of-sight, improve the comfort of the subject and the quality of the measurement. The fast acquisition with only one fixation target also decreases the impact of changes in fixation, accommodation, tear film, and muscle tension, which might have a negative impact on the measurements.

Measuring with high angular resolution improves the capacity to resolve differences in aberrations with eccentricity compared to situations where only one measurement is taken every 5 or 10 degrees. It also increases the reliability since in a normal eye the aberrations are not expected to change abruptly with one degree of eccentricity, e.g. the presence of a bump should be detected over various degrees. This makes the measurement of the shape of the relative peripheral refraction curve more robust against a few erroneous measurements.

The corneal reflection, as is known in any ocular Hartmann-Shack sensors applications, is a major problem when measuring the horizontal meridian with this instrument. The reflection of the beam on the anterior corneal surface can enter the measuring arm and distort the spot pattern. To deal with this problem we chose to keep the line-of-sight and the path of the entrance light parallel to each other but slightly moved in the vertical plane (Y-axis). For people with small pupils it is less easy to avoid the corneal reflection and it may result in the loss of some measurements. However, since the scanning resolution is high it is still possible to resolve the trend in the variation with eccentricity. Since the filtering that we use to detect the spots and the unwrapping algorithm are quite powerful they can handle the loss of spots due to the corneal reflection as long as the reflection does not saturates the camera making it impossible to see any spots or if the central spots are corrupted.

Alignment of the subject is critical for having good measurements. It is important to ensure that the centre of rotation of the instrument coincides with the pupil plane of the eye so that all measurements are taken in the same plane. Whether this is the exact plane of the entrance pupil at each eccentricity and what is the impact of a possible small mis-alignment on the coefficients of the Zernike polynomials is not yet quantified [27]. The choice of the algorithms used to process the HS-images could play an important roll to incorporate angular corrections when those small mis-alignments appear to be significant. During alignment, the 0° point of the instrument is aligned to the line-of-sight of the subject. Aligning the subject consumes the most time of the measuring procedure, especially when trying to avoid the corneal reflection. In general, for a trained operator, alignment takes about 1 minute. But this is not necessarily negative since the subjects can get familiar with the instrument and its movements while maintaining normal blinking habit during this time.

Comparing the aberrations measured with the new HS-scanner with those measured with the static HS sensor high correlation and no significant difference was found. But the acquisition time, the angular resolution and the comfort of the subject and operator were largely improved.

5. Conclusion

We have developed a unique instrument: a fast scanning HS wave-front sensor for measuring the optical quality in the periphery of the human eye. It is capable of measuring the eyes'

#140615 - $15.00 USD Received 5 Jan 2011; revised 23 Mar 2011; accepted 25 Mar 2011; published 8 Apr 2011

aberrations over the central 80° of the horizontal visual field in 1.8 seconds with an angular resolution of 1 measurement per degree. This high speed and large scanning angle can be reached because the system is based on a rotational movement, keeping the distance between the eye and the instrument equal at all angles. Due to careful optimization of the components, the instrument is rather compact and silent. Furthermore, the new design is comfortable for the subject due to the use of a head-chin rest and because no moving elements are in the line-of-sight of the subject. The instrument is mounted on an ophthalmic XYZ-bench which makes it possible for the operator to align the instrument to the subject with minimum disturbance. Changing the HS-wavefront sensor from a static to a scanning instrument had no negative effects on the measuring results as seen from the comparison study. The instrument has the capability to be used in a clinical environment or in population studies. Due to its characteristics it is perfectly suitable to be used in the investigation of myopia development and in the design of peripheral optical corrections. This system can be used in the future either for basic experiments on the optical properties of a large group of eyes in the periphery as in clinical application where the control or the modification of the peripheral eye's properties is required.

Acknowledgments

This work was supported by the "Ministerio de Educación y Ciencia," Spain (grant FIS2007-64765 and CONSOLIDER-INGENIO 2010, CSD2007-00033 SAUUL); Fundación Séneca (Region de Murcia, Spain), grant 4524/GERM/06; and by European Commission's sixth framework program through the Marie Curie Research Training Network MY EUROPIA (MRTN-CT-2006-034021). Author LL was also supported by the Swedish Agency for Innovation Systems (VINNMER 2008-00992).

#140615 - $15.00 USD Received 5 Jan 2011; revised 23 Mar 2011; accepted 25 Mar 2011; published 8 Apr 2011